Progress In Electromagnetics Research M, Vol. 72, 23–30, 2018

Design of a Dual-Polarized Broadband Single-Layer Reflectarray Based on Square Spiral Element

Yang Liu[1, 2, *], Hongjian Wang[1, 2], and Xingchao Dong[1, 2]

Abstract—A dual-polarized broadband single-layer reflectarray antenna based on square spiral element is presented in this paper. Two designs with similar square spiral structures but different construction processes and transition patterns are investigated and compared. The comparison results show that the design varying the length of the first stub of one-arm square spiral is more suitable for building the reflectarray. Several 441-element reflectarray antennas fed by horn with different offset angles are also simulated and compared to show the broadband characteristic. A reflectarray with offset angle of 15 degrees is then fabricated and tested. The measured results show good radiation performances, and the 1-dB gain bandwidth of 34.7% is obtained. The measured gain is 27.1 dB at the center frequency of 15 GHz, which is equivalent to 45.6% aperture efficiency.

1. INTRODUCTION

Reflectarray implemented in microstrip form exhibits numerous distinctive advantages such as low profile, low cost, light weight and easy fabrication [1, 2]. Many reflectarray antennas have been designed to realize the desired performances in recent years. Among all these designs, single-layer implementation, commonly using element structure of particular shape, is much easier to design and fabricate than multiple-layer implementation and will not degrade the bandwidth performance at the same time [3–6].

Square or circular patch, ring and their improvements [7–10] are the most common phasing elements used in a reflectarray, but the bandwidth performances are not so good, usually 10% or so when speaking of relative bandwidth. So new elements are searched for better bandwidth responses, and spiral elements show relatively good characteristics. Spiral element used in reflectarray is first introduced by Phelan in [11] to realize spiraphase using a 4-arm spiral element with switching diodes at center. However due to its large element size and spacing, the aperture efficiency of the antenna is relatively poor. The antenna is also heavy because of the biasing circuit. Four circular quasi-spiral lines attached to circular rings [12] are used as phase delay lines to achieve large phase range. The phase shift range of more than 1000° means that the reflection phase is sensitive to the change of spiral line, which requires finer fabrication. The measured 1-dB gain bandwidth of 16.5% of this design is achieved. Spiral stubs implemented in [13] are attached to a modified double square loop structure. By adjusting stub length, large phasing range of 420° can be attained whereas the reflection magnitude at some lengths is poor. Good bandwidth performance is obtained, and the 1-dB gain bandwidth of 38% is achieved. In [14], different from the former two mentioned papers, the Archimedes spirals are not attached to patch or ring structures. Only four Archimedes spirals are adopted to form the phasing element. This design achieves about 540° linear reflection phase range and good bandwidth performance. From the above papers, it can be concluded that spiral structure can realize large reflection phase range and relatively large bandwidth. Square

Received 2 July 2018, Accepted 6 August 2018, Scheduled 13 August 2018

* Corresponding author: Yang Liu (lyxyz1234@163.com).

[1] CAS Key Laboratory of Microwave Remote Sensing, National Space Science Center, Chinese Academy of Sciences, Beijing 100190, China. [2] University of Chinese Academy of Sciences, Beijing 100049, China.

spiral [15] is another kind of spiral lines which is studied in other antenna forms but has never been used in reflectarray.

Combining a square spiral and the configuration of four-arm Archimedes spirals [14], a novel reflectarray using a four-arm square spiral with a small aperture is first introduced in [16]. In this paper, the design details of the square spiral structure, especially the comparison of two different constructions, are provided. In Section 2, the implementation, transition and reflection responses of the two proposed square spiral elements are compared. Then, the reflectarray antennas with larger aperture under different feed angles are designed and compared for bandwidth performances. Besides, the measured results are presented in Section 3. Finally, the conclusions are given.

2. ELEMENT DESIGN AND COMPARISON

Differing from the formula-based Archimedes spiral described in [14], the square spiral is hard to express by simple equations related to its length. Therefore, the study of the reflection performances varying with one particular parameter is hardly carried out. In order to alleviate this problem, two square spiral structures with different construction methods are created, as shown in Fig. 1. The proposed two elements are mounted on a substrate F4B with permittivity of 2.25 and dielectric loss tangent of 0.001. Besides, the substrate thickness is optimized as $H = 3\,\text{mm}$ [16]. The stub width w is 0.5 mm, and the gap s between two arms is 0.3 mm. The unit cell periodicity is $P = 0.45\lambda_0 = 9\,\text{mm}$, where λ_0 is the free-space wavelength at the center frequency of 15 GHz.

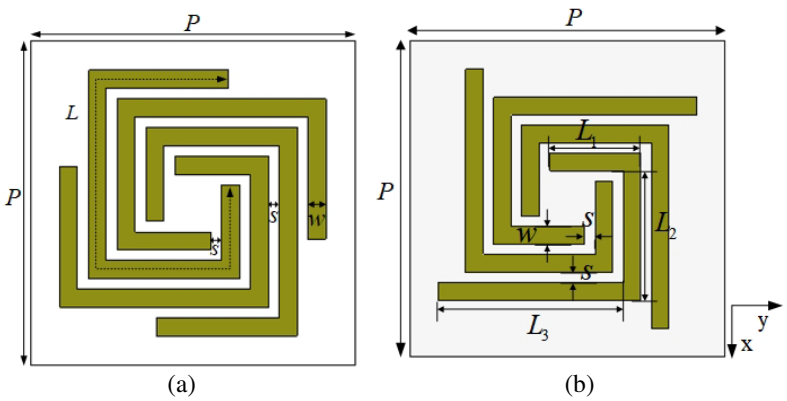

Figure 1. The top view of the two designs using square spiral structure. (a) Design I. (b) Design II.

According to the general method of designing reflectarray, the database of the element performance with sweeping parameter should be established first by simulation in full-wave simulation software, such as HFSS adopted in this design.

In Design I, the total length of one-arm square spiral L is utilized as the primary changing factor to prolong the structure. This structure changing method is similar to the simulation approach in [14]. For lack of corresponding equations, a sophisticate modeling process is performed in HFSS to automatically work on the turning of the square spiral, as illustrated in Fig. 2. Specifically, four stubs (the blue parts) with length of L are lengthened from four different positions, and then they intersect with the corresponding stubs of the complete square spiral structure (the orange part). Obviously, the extra parts will be removed, and the remaining intersection part (the brown part) is the needed structure with length of L. The brown part coverage will expand, and the orange part will decrease when L increases. In Design II, each square spiral arm unites three rectangular stubs end to end, and the latter stub is perpendicular to the previous one. The lengths of the three stubs are L_1, L_2 and L_3, respectively. The relations of these parameters are as follows: $L_2 = L_1 + w + 2\,s$, $L_3 = L_2 + 2\,(s + w)$. The phase shift is obtained by adjusting the first stub length L_1. It should be noted that the other two stubs are altered simultaneously, which means that the whole structure is expanding outwards. From the perspective of design complexity, it will take less time to construct the whole reflectarray if Design II is employed.

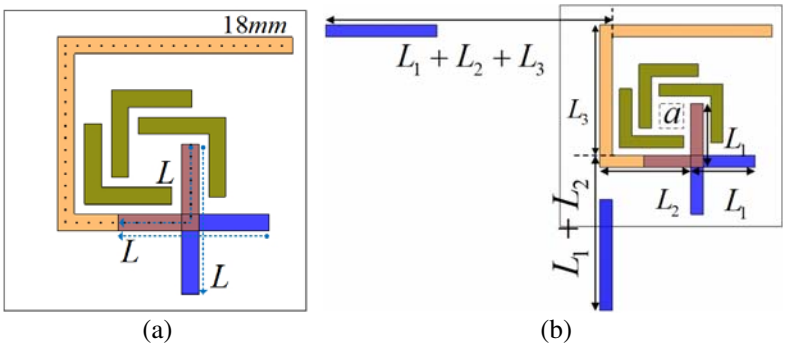

Figure 2. The construction demonstration of Design I. (a) Partial view. (b) Global view. Dimensions are as follows: $a = 1$ mm, $L_1 = a + 2(w + s)$, $L_2 = L_1 + w + 2s$, $L_3 = L_2 + 2(w + s)$.

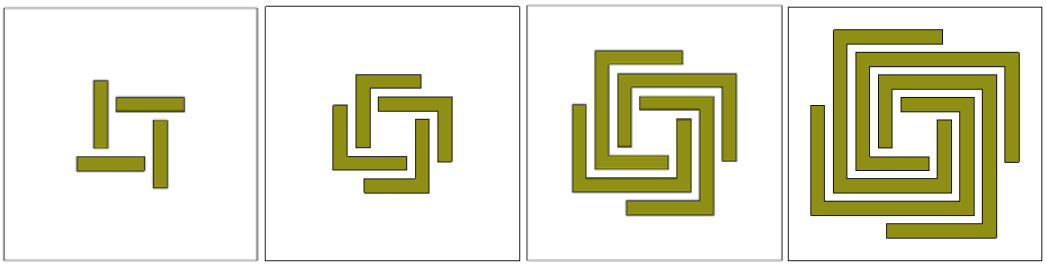

Figure 3. The structure transitions of the Design I. (a) L = 1–2.6 mm. (b) L = 2.6–6.3 mm. (c) L = 6.3–11.6 mm. (d) L = 11.6–18 mm.

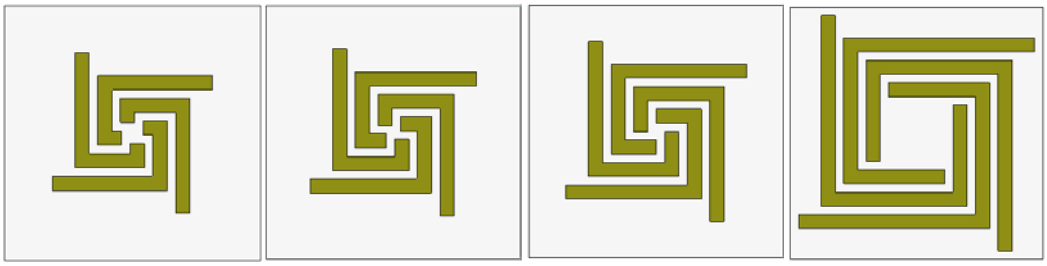

Figure 4. The structure transitions of the Design II. (a) L_1 = 0.85 mm. (b) L_1 = 1.1 mm. (c) L_1 = 1.6 mm. (d) L_1 = 3.6 mm.

Transition diagrams of the unit cell in Design I and II are shown in Fig. 3 and Fig. 4, respectively. It can be observed that the one-arm square spiral is changed from one stub to three stubs in Design I, whereas the structure in Design II just keeps the initial pattern (each arm is composed of three stubs) and expands outwards. In addition, the starting location of square spiral in Design I is fixed during the changing period. By contrast, the origin of square spiral in Design II floats with the increase of the first stub.

The reflection performances simulated in HFSS with Flouquet port excitations and master-slave boundaries are also analyzed and compared. Fig. 5 shows the reflection results of Design I and II at 14, 15 and 16 GHz. It can be seen that the reflection phase curves at different frequencies are approximately parallel to each other in both designs, which indicates good bandwidth potential. The difference between the two designs is the reflection phase shift range. The reflection phase range is about 560° in Design I when the square spiral length changes from 1 mm to 18 mm. On the other hand, the phase range about

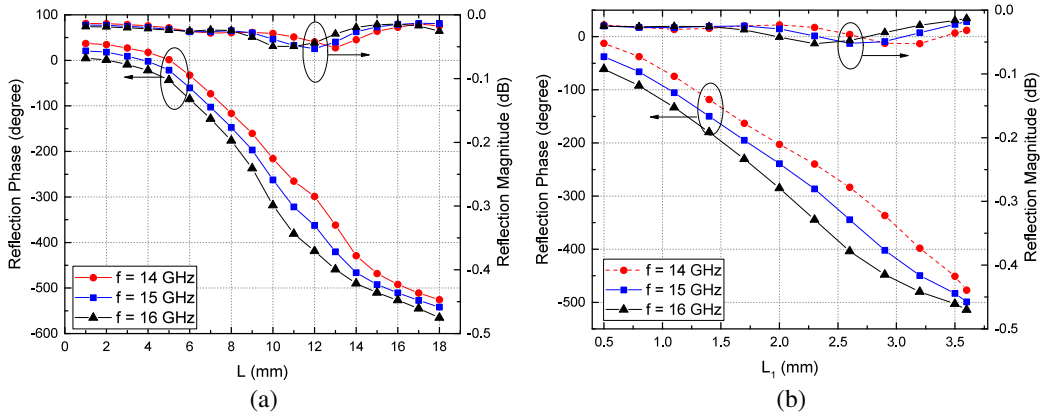

Figure 5. The re ection responses for different frequencies. (a) Design I. (b) Design II.

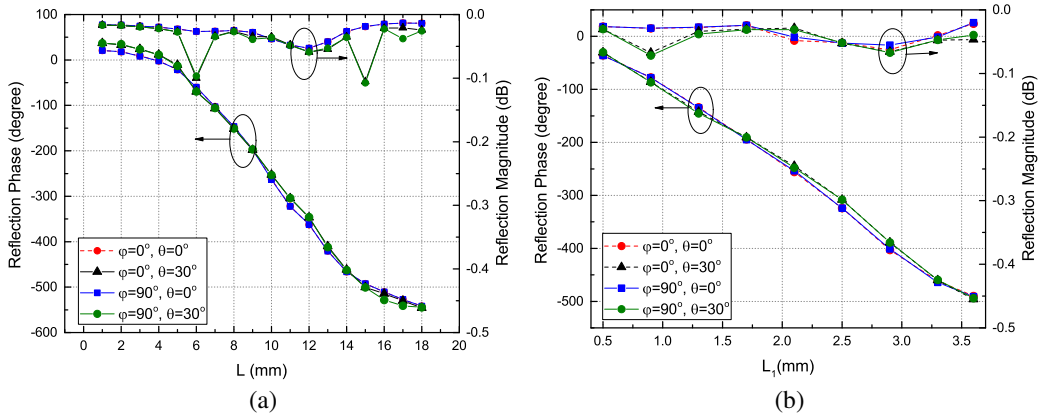

Figure 6. The re ection responses for different incident angles. (a) Design I. (b) Design II.

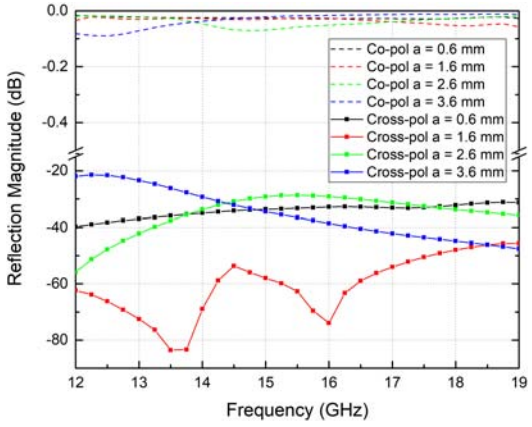

Figure 7. The co- and cross-polarization of element in Design II.

460° is obtained in Design II within the sweeping scope. Both designs apparently satisfy the phase range requirement of 360°, and about 100° phase shift range difference may not affect the reflectarray performance dramatically. The simulated reflection responses for oblique incidence at center frequency are also examined, and the results are illustrated in Fig. 6. It is obtained that the phase curves for different angles of incidence are mostly overlapped in both designs, which means that the incident angle has little influence on phase shifting.

Given the design complexity and reflection performances of Design I and II, we choose Design II as an example to fabricate and verify the performance. The cross-polarized components of the element in Design II are displayed in Fig. 7, which shows the ability of dual linear polarizations.

3. REFLECTARRAY DESIGN AND PERFORMANCES

In order to verify the performance of the proposed square spiral element in Design II, the single-layer microstrip reflectarray is then designed. The required phase distribution can be determined theoretically by the following Equation (1):

$$\Phi_R = k_0 \cdot (d_i - (x_i \cos\phi_b + y_i \sin\phi_b) \sin\theta_b)) \tag{1}$$

where k_0 is the propagation constant in free space, d_i the distance from the phase center of the feed to the center of each unit cell, and (θ_b, ϕ_b) the designed main beam direction of the reflectarray. Considering the limited configuration of the computer, only 441 elements are used to form the reflectarray, and every two adjacent elements are arranged symmetrical to the centerline between them to reduce the cross-polarization level [17]. The square aperture D is 189 mm, and the focal length $F = D$. The reflectarray is fed by a linearly polarized pyramid horn with gain of 15.2 dB. The radiation patterns of the feed horn are shown in Fig. 8. The offset angle of the feed is studied first. Several reflectarrays with different angles offseting the broadside direction are designed and simulated. The result comparisons are shown in Fig. 9, and the 1-dB gain bandwidths are calibrated in Table 1. We can see that the simulated 1-dB gain bandwidths are about 29–39% with different offset angles. At this 441-element reflectarray configuration, the 1-dB gain bandwidth around 30% remains relatively stable.

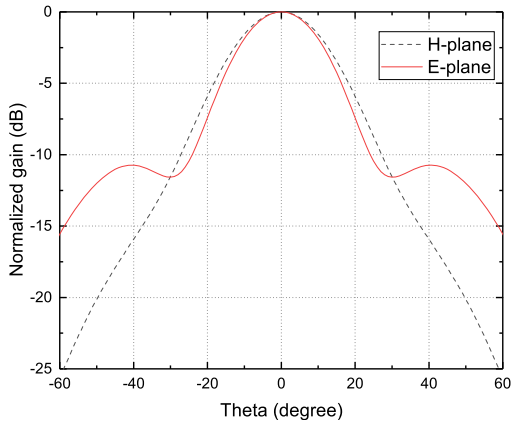

Figure 8. The radiation patterns of the feed horn.

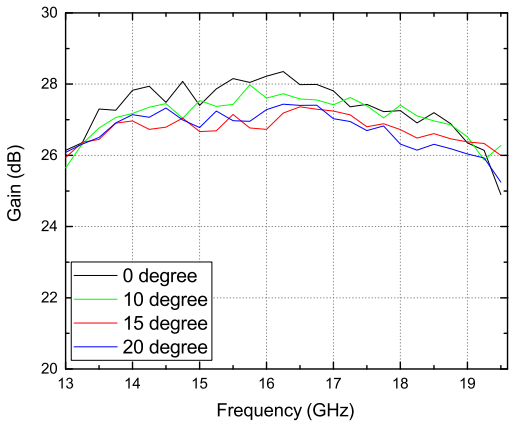

Figure 9. The gain performances under different incident angles.

Table 1. The 1-dB gain bandwidth performances with different offset angles

Offset Angle	0°	10°	15°	20°
1-dB Gain Bandwidth	29.3%	30.7%	39.3%	31.3%

A reflectarray with fed angle of 15 degrees is fabricated as a verification example, as shown in Fig. 10(a). The reflectarray is measured in a microwave anechoic chamber employing NSI2000 system. The normalized radiation patterns of co-polarization and cross-polarization in E-plane and H-plane at center frequency of 15 GHz are presented in Fig. 11(a) and Fig. 11(b), respectively. The performances of the designed antenna can be obtained from these patterns. The measured sidelobe level (SLL) is about -19 dB in E-plane and -21 dB in H-plane. The cross polarization level (CPL) is about -31 dB in E-plane and -29 dB in H-plane. As shown in Fig. 11(a), the mainbeam of radiation pattern in E-plane is

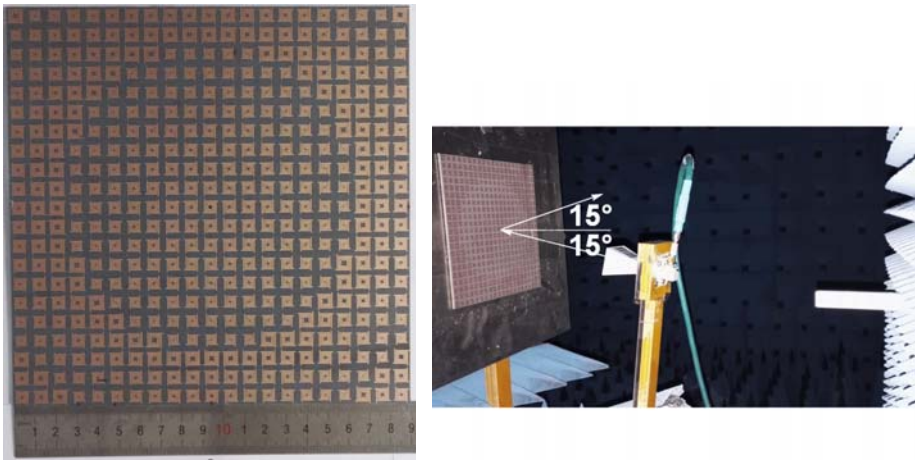

(a) (b)

Figure 10. The prototype of fabricated reflectarray. (a) Top view. (b) Under test.

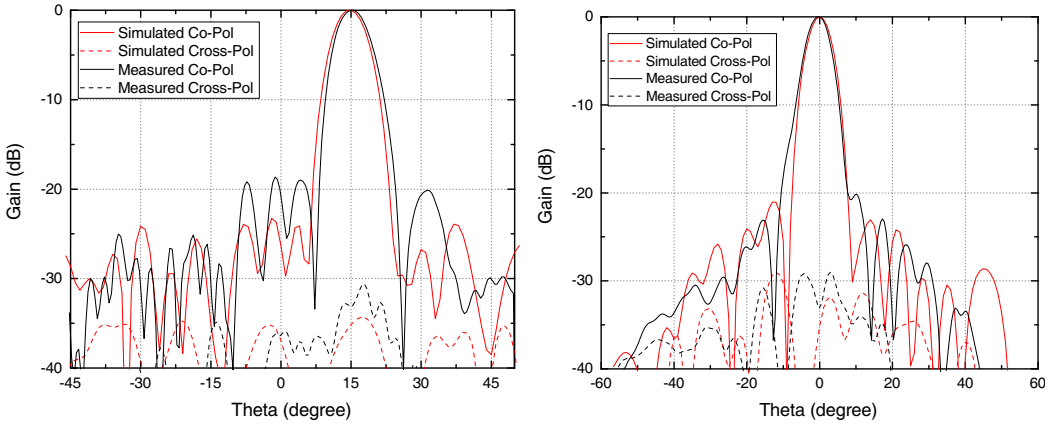

(a) (b)

Figure 11. Simulated and measured radiation patterns. (a) E-plane. (b) H-plane.

toward the desired direction tilted exactly 15° from the normal direction of the reflectarray. Additionally, the SLL of the measured radiation pattern in E-plane is about 5 dB higher than the simulated pattern at 15 GHz. This may be mainly caused by the deformation of the microstrip reflectarray and the misalignment of the feed horn during test. That is to say, the horn aperture is not perpendicular to the 15 degree line offset from the broadside direction. From the horn radiation patterns shown in Fig. 8, it is clear that the side lobe is high in E-plane. It can also be noted that good agreement between the simulated and measured results is obtained in the corresponding H-plane, as demonstrated in Fig. 11(b).

Meanwhile, the measured radiation patterns in both principal planes of the reflectarray at different frequencies are also given. Fig. 12(a) displays the co-polarized and cross-polarized radiation patterns in E-plane when the frequency varies from 14 GHz to 19 GHz. Similarly, Fig. 12(b) shows the co-polarized and cross-polarized radiation patterns in H-plane at the frequencies of 14–19 GHz. It is concluded that the radiation patterns at the frequency band of interest maintain the well-defined pencil beam. Though the SLL at some frequency is as high as −15 dB, the SLLs in most of the radiation patterns are around −20 dB.

The measured gain and aperture efficiency of the designed reflectarray within the frequency band of interest are also displayed in Fig. 13. The measured gain is 27.1 dB at center frequency of 15 GHz, and the maximum gain is 27.8 dB, which is obtained at 17.6 GHz. The 1-dB gain bandwidth is about 34.7% from 13.9 GHz to 19.1 GHz. The aperture efficiency is important for planar aperture antenna [18], and

it can be calculated by

$$\eta_a = \frac{G\lambda^2}{4\pi A} \tag{2}$$

where $A = D^2$ denotes the physical area of the reflectarray aperture, and G is the measured gain. D is the side length of the square aperture of the reflectarray. The aperture efficiency is around 46% at the neighbor band of central frequency. According to Eq. (2), if the measured gain remains constant in a large scope of frequency band, the aperture efficiency will decrease for certain when the frequency increases.

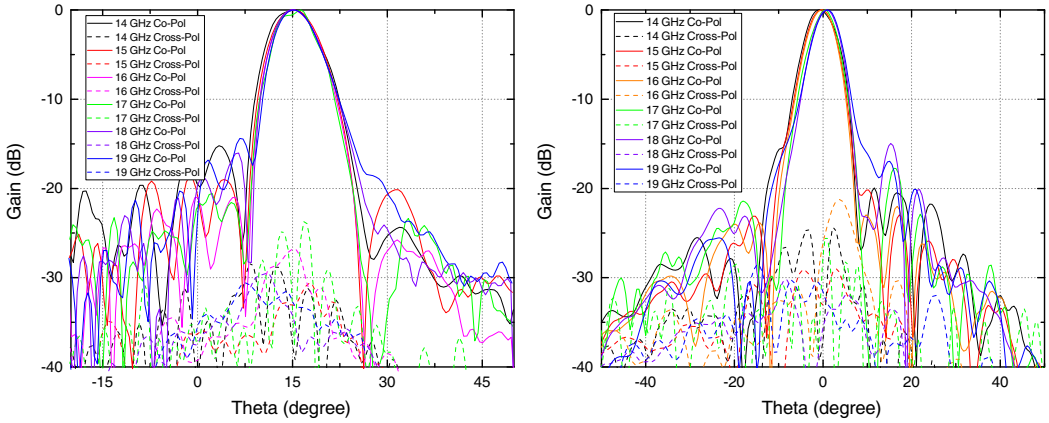

Figure 12. Measured radiation patterns. (a) E-plane. (b) H-plane.

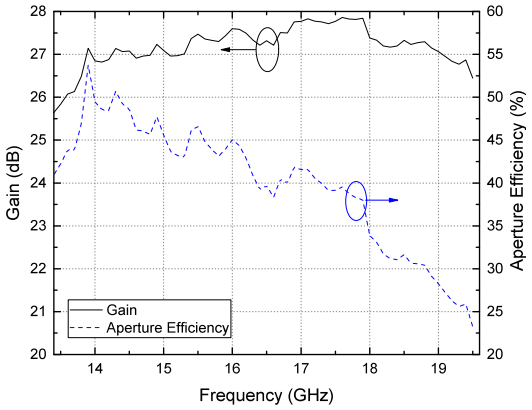

Figure 13. The gain and aperture efficiency versus frequency.

4. CONCLUSIONS

A dual-polarized single-layer reflectarray using a square spiral element has been described. The detailed comparisons are performed between the two designs with different ways of sweeping and changing patterns. The design of sweeping first stub length of square spiral is chosen, and several refletarray antennas with different fed angles are designed for the comparisons of bandwidth performances. A reflectarray with a square aperture of 189 mm and an offset angle of 15° is fabricated and tested. The gain of 27.1 dB and 1-dB gain bandwidth of 34.7% are achieved at center frequency of 15 GHz, which indicate that the proposed design is suitable for broadband situation.

REFERENCES

1. Huang, J. and J. A. Encinar, *Reflectarray Antennas*, John Wiley and Sons Inc, Hoboken, NJ, USA, 2007.
2. Shaker, J., M. R. Chaharmir, and J. Ethier, *Reflectarray Antennas: Analysis, Design, Fabrication, and Measurement*, Artech House, Norwood, MA, USA, 2013.
3. Bialkowski, M. E. and K. H. Sayidmarie, "Investigations into phase characteristics of a single-layer reflectarray employing patch or ring elements of variable size," *IEEE Transactions on Antennas and Propagation*, Vol. 56, No. 11, 3366–3372, 2008.
4. Abdelrahman, A. H., A. Z. Elsherbeni, and F. Yang, "High-gain and broadband transmitarray antenna using triple-layer spiral dipole elements," *IEEE Antennas and Wireless Propagation Letters*, Vol. 13, 1288–1291, 2014.
5. Qin, P. Y., Y. J. Guo, and A. R. Weily, "Broadband reflectarray antenna using subwavelength elements based on double square meander-line rings," *IEEE Transactions on Antennas and Propagation*, Vol. 64, No. 1, 378–383, 2016.
6. Liu, Y., H. Wang, F. Xue, and X. Dong, "A new single-layer reflectarray using circular patch with semicircular ring slots," *Progress In Electromagnetics Research Letters*, Vol. 66, 105–111, 2017.
7. Malfajani, R. S. and Z. Atlasbaf, "Design and implementation of a broadband single layer circularly polarized reflectarray antenna," *IEEE Antennas and Wireless Propagation Letters*, Vol. 11, 973–976, 2012.
8. Guo, L., P. K. Tan, and T. H. Chio, "A simple method to realize polarization diversity in broadband reflectarrays using single-layered rectangular patch elements," *Proc. IEEE Int. Symp. Antennas and Propagation USNC/URSI National Radio Science Meeting*, 2161–2162, 2015.
9. Ortiz-Fuentes, J. A., J. Silva-Montero, J. I. Martinez-Lopez, J. Rodriguez-Cuevas, and A. E. Martynyuk, "Dual-frequency reflectarray based on split ring slots," *IEEE Antennas and Wireless Propagation Letters*, 99, 2016.
10. Han, C., Y. Zhang, and Q. Yang, "A broadband reflectarray antenna using triple gapped rings with attached phase-delay lines," *IEEE Transactions on Antennas and Propagation*, Vol. 65, No. 5, 2713–2717, 2017.
11. Phelan, H. R., "Spiraphase reflectarray for multitarget radar," *Microwave Journal*, Vol. 20, 67, 1977.
12. Derafshi, I., N. Komjani, and M. Mohammadirad, "A single-layer broadband reflectarray antenna by using quasi-spiral phase delay line," *IEEE Antennas and Wireless Propagation Letters*, Vol. 14, 84–87, 2015.
13. Wang, Q., Z. H. Shao, Y. J. Cheng, and P. K. Li, "Broadband low-cost reflectarray using modified double-square loop loaded by spiral stubs," *IEEE Transactions on Antennas and Propagation*, Vol. 63, No. 9, 4224–4229, 2015.
14. Xue, F., H. J. Wang, M. Yi, G. Liu, and X. C. Dong, "Design of a broadband single-layer linearly polarized reflectarray using four-arm spiral elements," *IEEE Antennas and Wireless Propagation Letters*, Vol. 16, 696–699, 2017.
15. Wei, H., M. Lin, and Y. Xiang, "Compact square spiral printed antenna," *Electronics Letters*, Vol. 50, No. 3, 135–136, 2014.
16. Liu, Y., H. Wang, F., Xue, and X. Dong, "A novel single-layer reflectarray antenna using square spiral element," *Proc. IEEE Int. Symp. Antennas and Propagation USNC/URSI National Radio Science Meeting*, 95–96, 2017.
17. Hasani, H., M. Kamyab, and A. Mirkamali, "Low cross-polarization reflectarray antenna," *IEEE Transactions on Antennas and Propagation*, Vol. 59, No. 5, 1752–1756, 2011.
18. Morabito, A. F., "Synthesis of maximum-efficiency beam arrays via convex programming and compressive sensing," *IEEE Antennas and Wireless Propagation Letters*, Vol. 16, 2404–2407, 2017.